IOP Conf. Series: Materials Science and Engineering **266** (2017) 012001 doi:10.1088/1757-899X/266/1/012001

Nucleation and microstructure development in Cr-Mo-V tool steel during gas atomization

M Behúlová, P Grgač and R Čička

Slovak University of Technology in Bratislava, Faculty of Materials Science and Technology in Trnava, Ulica Jána Bottu č. 2781/25, 917 24 Trnava, Slovakia

maria.behulova@stuba.sk

Abstract. Nucleation studies of undercooled metallic melts are of essential interest for the understanding of phase selection, growth kinetics and microstructure development during their rapid non-equilibrium solidification. The paper deals with the modelling of nucleation processes and microstructure development in the hypoeutectic tool steel Ch12MF4 with the chemical composition of 2.37% C, 12.06 % Cr, 1.2% Mo, 4.0% V and balance Fe [wt. %] in the process of nitrogen gas atomization. Based on the classical theory of homogeneous nucleation, the nucleation temperature of molten rapidly cooled spherical particles from this alloy with diameter from 40 μm to 600 μm in the gas atomization process is calculated using various estimations of parameters influencing the nucleation process – the Gibbs free energy difference between solid and liquid phases and the solid/liquid interfacial energy. Results of numerical calculations are compared with experimentally measured nucleation temperatures during levitation experiments and microstructures developed in rapidly solidified powder particles from the investigated alloy.

1. Introduction

Nucleation studies in the undercooled metallic melts are of essential interest for the understanding of phase selection and microstructure development. In addition to the knowledge of growth kinetics, the understanding of nucleation phenomena is an important ingredient for the interpretation of metastable phases formation because of its significant influence on the initial stage of solidification [1-6].

During the past decades, the positive consequences of rapid solidification of melts have been successfully applied in several progressive technologies of production and treatment of materials, e. g. solidification on cooling substrates, gas and water atomization techniques, plasma spray deposition, local surface laser or electron beam melting, etc.

High cooling rates of the melt enable to attain large melt undercoolings below the equilibrium liquidus temperature [7-9]. Consequently, deep initial undercoolings initiate high velocities of solid-liquid (S-L) interface and create conditions for the development of a great variety of materials with chemical compositions, solidification microstructures and properties which are impossible to produce by conventional metallurgical technologies. Generally, the increase in initial melt undercooling leads to the enhancement of homogeneity of solid phase, microstructure refinement, to the formation of metastable crystalline and quasi-crystalline phases, and also metallic glasses [1,10-11].

Introduced benefits of rapid solidification processing result from transition from equilibrium or quasi-equilibrium solidification in bulk volumes of melt to the rapid non-equilibrium solidification in spatially limited ranges by high S-L interfacial velocities. The development of final solidification

microstructures is determined particularly by thermodynamic and thermokinetic conditions of rapid cooling, nucleation and solidification of melt [12-13].

Tool steels of ledeburite type (high chromium and high speed steels) form a group of alloys produced by powder metallurgy by the gas atomization of melt followed by consolidation of rapidly solidified (RS) particles. They are characteristic by the high wear resistance caused by the carbide phases of solidification origin present in their microstructure.

Generally, the cooling and solidification of molten droplets in atomization process proceeds in several stages: rapid cooling, nucleation, rapid crystal growth during recalescence (quasi-adiabatic solidification), quasi-isothermal period of structure development in the semi-solidified particle and the cooling of solidified particle. In this paper, the nucleation temperature of molten rapidly cooled spherical particles from the Ch12MF4 tool steel in the gas atomization process is predicted on the base of classical theory of homogeneous nucleation. The influence of initial melt undercooling bellow the equilibrium liquidus temperature on the final microstructure development in the powder particles of different diameters is discussed.

2. Experimental materials and methods

For experimental measurements and theoretical study, two similar high alloyed tool steel of ledeburite type were applied, namely, the Ch12MF4 tool steel in the form of powder prepared by nitrogen gas atomisation and its equivalent K190 Isomatrix from BÖHLER Edelstahl GmbH company. The chemical composition of experimental steels is given in Table 1.

Table 1. Chemical composition of investigated steels.

Steel grade	Element [wt. %]					
	C	Cr	Mo	V	Si	Fe
Ch12MF4	2.37	12.06	1.2	4.0	-	bal.
K 190 Isomatrix	2.3	12.5	1.1	4.0	0.4	bal.

The process of quasi-equilibrium solidification of the Ch12MF4 steel was experimentally investigated using differential thermal analysis (DTA). In addition, material properties and solidification characteristics were computed by ThermoCalc and JMatPro software [14, 15]. According to DTA measurements and computed results, solidification of the Ch12MF4 steel in quasi-equilibrium conditions is initiated at the liquidus temperature of 1324 °C by the austenite crystallization followed by two eutectic reactions. The first eutectic reaction starts at the temperature T_{E1} = 1253 °C. During this eutectic reaction, the growth of two-phase mixture of austenite and MC carbides occurs. At the temperature T_{E2} = 1239 °C, the second eutectic reaction begins, which results in the formation of another two-phase mixture of austenite and M_7C_3 carbides. The process of quasi-equilibrium solidification is finished at the solidus temperature of 1225 °C. The phase identification was performed by transmission Mössbauer spectrometry and X-ray diffraction analysis [16-17].

Rapidly solidified (RS) powder particles of Ch12MF4 steel were screened into nine standard size granulometric fractions ranging from 50 μm to 56 μm up to more than 630 μm. The analysis of solidification microstructures developed in powder particles during non-equilibrium solidification was carried out using light microscopy (LM), scanning (SEM) and transmission electron microscopy (TEM).

To investigate the temperatures of spontaneous nucleation in the K190 Isomatrix alloy experimentally, the levitation techniques were exploited.

3. Solidification microstructures in rapidly solidified powders

A detailed analysis of solidification microstructures in 500 RS particles from each size fraction was performed [18]. The total number of 4500 particles was observed and analyzed. From the morphological point of view, three main types of solidification microstructures were identified RS powder particles (Figure 1): dendritic, cellular (grain-refined) and compound, representing the mixture of dendritic and cellular microstructures. The percentage population of the main types of solidification microstructures

in analyzed granullometric fractions of RS powder is shown in Figure 2. Dendritic microstructure represents the dominant morphological variant in RS particles. It was found in each granullometric fraction while its percentage population decreased with the increase in particle size. On the other hand, the percentage population of compound and cellular (grain-refined) microstructures increases for the larger granullometric fractions. The considerable enhancement in percentage population of these microstructures was registered in the granullometric fractions larger than 125–168 µm. The appearance of cellular microstructures on a statistically significant scale was identified in the particles from the size fraction of 71-80 µm.

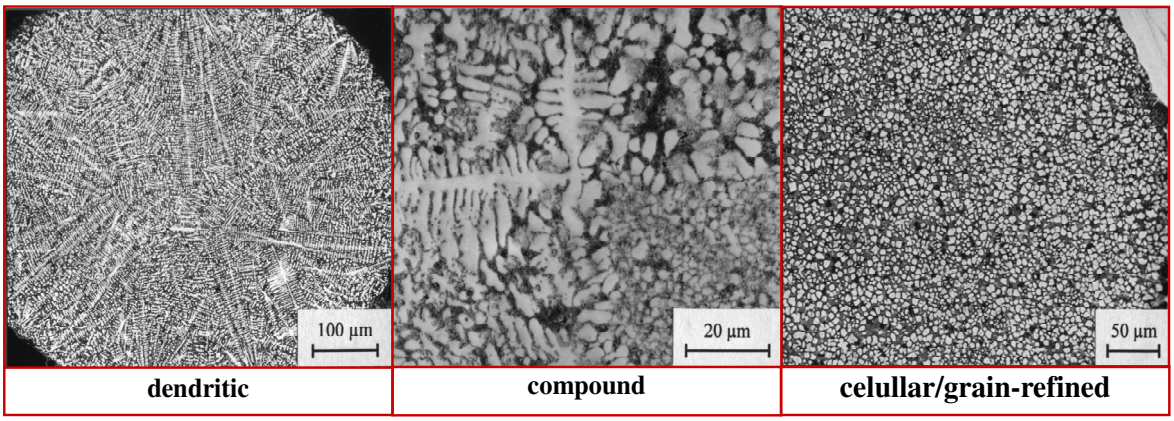

Figure 1. Main types of solidification microstructures identified in RS particles of the Ch12MF4 steel: dendritic, compound and cellular (grain refined).

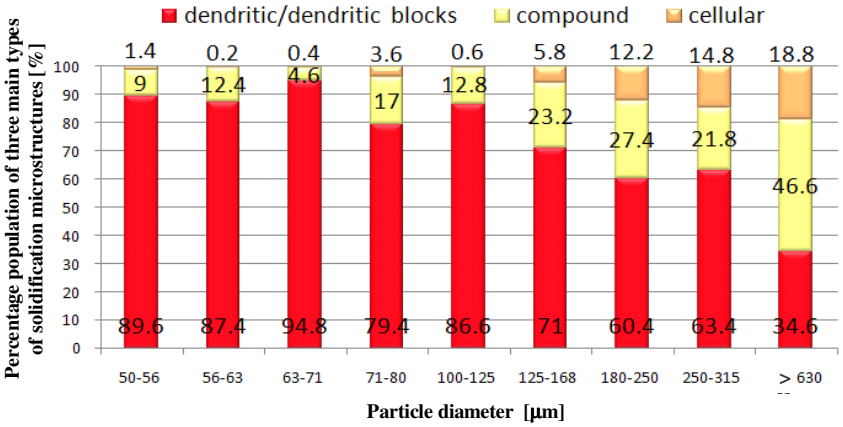

Figure 2. Percentage population of the main types of solidification microstructures identified in analyzed granullometric fractions of RS powder [18].

Based on the performed microstructural analysis it is supposed that the transition from dendritic to compound and cellular (grain-refined) microstructure occurs by the mechanism of thermally induced fragmentation of primary dendrites developed during the initial phase of solidification and following spheroidization of dendrite fragments during the quasi-isothermal period of solidification [17]. The time–temperature–microstructure model of the microstructure development in the rapidly solidified powder particles of Ch12MF4 steel was proposed [18] on the base of results of microstructural analyses and simulation model of the process of single droplet cooling and solidification during gas atomization. There was supposed in the simulation model that the process of droplet solidification starts from the multiple nucleation evens by the nucleation at the defined nucleation temperature from the interval from

1000 °C to 1300 °C corresponding to the initial melt undercooling below the equilibrium liquidus temperature from 324 K to 24 K. The influence of the nitrogen gas velocity, particle size and nucleation temperature on the thermal history of droplets during atomization was studied [18]. According to obtained results, the nucleation temperature has a crucial effect on the computed recalescence temperature and duration of quasi-isothermal period of solidification. From the microstructural point of view, these parameters are responsible for the formation of different morphological variants of solidification microstructures developed in RS powder particles of Ch12MF4 steel.

In this reason the following research was focused on the identification of the maximum possible undercooling before the nucleation, which can be attained in the droplets from Ch12MF4 steel with different diameters during gas atomization. Using the classical theory of homogeneous nucleation, the nucleation temperature of molten rapidly cooled spherical particles from this alloy with diameter from 40 μm to 600 μm in the gas atomization process was calculated using various estimations of parameters influencing the nucleation process. Moreover, the levitation experiments were conducted to measure the reachable undercooling in the melt of the alloy with similar chemical composition.

4. Mathematical model

According to the newtonian conditions, the thermal history of a spherical droplet can be described by the heat balance equation. The enthalpy decrease with time is equal to the heat extracted per time unit from the droplet surface to the surroundings [19]

$$-\frac{\mathrm{d}H}{\mathrm{d}t} = h\left(T - T_{\mathrm{f}}\right)S \tag{1}$$

The heat removed through the droplet surface S depends on the combine heat transfer coefficient h and the temperature of atomizing gas T_{f}. Taking into account the enthalpy change of liquid and solid phases and the latent heat released, the time variation of the droplet temperature becomes

$$\frac{\mathrm{d}T}{\mathrm{d}t} = \left[-\frac{6h\left(T - T_{\mathrm{f}}\right)}{d} + \rho_{\mathrm{L}} l_{\mathrm{t}} \frac{\mathrm{d}f_{\mathrm{S}}}{\mathrm{d}t}\right]\left[\rho_{\mathrm{S}} c_{\mathrm{C}} f_{\mathrm{S}} + \rho_{\mathrm{L}} c_{\mathrm{L}}\left(1 - f_{\mathrm{S}}\right)\right]^{-1} \tag{2}$$

where d is the droplet diameter, ρ and c are the density and specific heat of solid (index S) and liquid (index L) phases, respectively, l_{t} is the latent heat and f_{S} is the solid fraction.

Solution of the equation (2) requires definition of geometrical, physical, initial and boundary conditions. The crucial problem consists in determination of cooling conditions, i. e. evaluation of the temperature and time dependent heat transfer coefficient during the droplet cooling by mechanisms of convection and radiation, determination of nucleation temperature and the velocity of solid-liquid (S-L) interface in the dependence on the melt undercooling.

Supposing the heat extraction from the droplet surface by convection and radiation, the boundary condition of the 3rd type [19] can be written in the form

$$-\lambda\left(grad\,T\right)_{\mathrm{w}} = h\left(T_{\mathrm{w}} - T_{\mathrm{f}}\right) \tag{3}$$

where T_{w} is the droplet surface temperature and λ is the thermal conductivity. Considering the energy losses to the surroundings characterized by the coefficient γ, the gas temperature can be determined from the equation

$$T_{\mathrm{f}} = T_{\mathrm{f0}} + \int_{T_0}^{\mathrm{T}} \left(1 - \gamma\right)\frac{\dot{m}c}{\dot{m}_{\mathrm{f}} c_{\mathrm{f}}}\mathrm{d}T \tag{4}$$

where $\dot{m} / \dot{m}_{\mathrm{f}}$ is the melt to gas mass flow ratio, c and c_{f} are specific heat capacities of alloy and gas, respectively and T_{f0} is the gas initial temperature.

The combined heat transfer coefficient h represents the sum of the convection heat transfer coefficient h_K and the equivalent radiation heat transfer coefficient h_R, $h = h_K + h_R$. Using the Ranz-Marshall criterial equation [19], the heat transfer coefficient can be determined from the relationship

$$h = h_K + h_R = \frac{\lambda_f}{d}\left[2 + 0.6\, Re^{1/2}\, Pr^{1/3}\right] + \varepsilon\sigma_0\left(T^2 + T_f^2\right)\left(T + T_f\right) \tag{5}$$

where Re is the Reynolds number, Pr is the Prandtl number, λ_f is the gas thermal conductivity, ε is the droplet emissivity and σ_0 represents the Stefan-Boltzmann constant.

The convection heat transfer coefficient depends particularly on the Reynolds number and relative velocity of the gas and droplet [20].

In order to determine the maximal possible droplet undercooling prior to solidification and to study the limiting conditions of droplet crystallization, homogeneous nucleation in the undercooled droplets is assumed. Nucleation occurs at the temperature T_N in the moment when one stable nucleus of critical size is created in the molten droplet with the volume V [7, 8]

$$N = V\int_{T_L}^{T_N}\frac{J_v(T)\,dT}{\dot{T}} = 1. \tag{6}$$

The symbol $\dot{T}$ denotes the cooling rate and $J_v(T)$ is the steady-state volumetric nucleation rate given by the relationship

$$J_v = \Omega_v\, exp\left(\frac{\Delta G^*}{k_B T}\right) \tag{7}$$

where ΔG^* is the activation barrier for nucleation, k_B is the Boltzmann constant and Ω_v is the preexponential factor with the value of 10^{35} cm^{-3}s^{-1} suggested by Perepezko [21] or $\Omega_v = 10^{30}/\eta$ [cm^{-3}s^{-1}] according to Thurnbull [22]. In this case Ω_v is the function of dynamic viscosity which can be for undercooled melts estimated from the relationship [23]

$$\eta = 10^{-3.3}\, exp\left[3.34 T_L/\left(T - T_g\right)\right] \qquad \text{[poise]} \tag{8}$$

Supposing formation of a spherical nucleus, the activation energy ΔG^* can be calculated as [61]

$$\Delta G^* = \frac{16}{3}\frac{\pi\sigma^3}{\Delta G_v^2} \tag{9}$$

where σ is the solid/liquid interfacial energy and ΔG_v is the difference of Gibbs free enthalpy of liquid and solid phases per unit volume. Both of these parameters have significant influence on calculated nucleation temperatures. Several authors have tried to estimate them by different mathematical approximations [25]. In this work, the interfacial energy is calculated using the relationship introduced by Thompson and Spaepen [23]

$$\sigma = \frac{\alpha\,\Delta S_m T}{\left(N_A V_m^2\right)^{1/3}} \tag{10}$$

where α is a structure dependent constant ($\alpha = 0.71$ for b.c.c. and $\alpha = 0.86$ for f.c.c./h.c.p.), ΔS_m is the molar entropy of fusion, N_A is the Avogadro number and V_m the molar volume.

The Gibbs free energy difference between solid and liquid phases ΔG_v, is given by the relationship

$$\Delta G_v = \frac{\Delta H_v \Delta T}{T_L} - \int_T^{T_L}\Delta c_p\, dT + T\int_T^{T_L}\frac{\Delta c_p}{T}\, dT \tag{11}$$

in which ΔH_v is the volumetric enthalpy of fusion (volumetric latent heat), Δc_p is the heat capacity difference between undercooled liquid and solid phases and $\Delta T = T_L - T$ is the melt undercooling.

As the experimental values of ΔG_v and Δc_p, respectively, are not available, their temperature dependences are approximated assuming various forms of Δc_p. For example, Thurnbull [10] proposed $\Delta c_p = 0$ for pure metals leading to the linear dependence of ΔG_v on the melt undercooling. Selected approximations for the computation of Gibbs free energy difference between solid and liquid phases ΔG_v are summarized in Table 2. All considered expressions for ΔG_v are related to the linear approximation of Turnbull through some correction factors.

Table 2. Selected approximations for the computation of Gibbs free energy difference ΔG_v.

Author(s)	Approximation of ΔG_v	Reference
Turnbull	$\Delta G_v = \frac{\Delta H_v \Delta T}{T_L}$	[26]
Hoffman	$\Delta G_v = \frac{\Delta H_v \Delta T}{T_L}\left(\frac{T}{T_L}\right)$	[27]
Thompson and Spaepen	$\Delta G_v = \frac{\Delta H_v \Delta T}{T_L}\left(\frac{2T}{T_L + T}\right)$	[28]
Battezzati and Garrone	$\Delta G_v = \frac{\Delta H_v \Delta T}{T_L} - 0.8\frac{\Delta H_v}{T_L}\left(\Delta T - T\, ln\frac{T_L}{T}\right)$	[29]
Jones and Chadwick	$\Delta G_v = \frac{\Delta H_v \Delta T}{T_L} - \frac{\Delta c_p^L (\Delta T)^2}{(T_L + T)}$	[30]
Dubey and Ramachandrarao	$\Delta G_v = \frac{\Delta H_v \Delta T}{T_L} - \frac{\Delta c_p^L (\Delta T)^2}{2T}\left(1 - \frac{\Delta T}{6T}\right)$	[31]
Singh a Holz	$\Delta G_v = \frac{\Delta H_v \Delta T}{T_L}\frac{7T}{T_L + 6T}$	[32]

Δc_p^L is the difference of thermal capacity between solid and liquid phases at the liquidus temperature

5. Results and discussion

The theory of homogenous nucleation was applied to predict achievable levels of undercooling of the spherical droplets from Ch12MF4 steel with diameters from 20 µm to 600 µm in the process of nitrogen gas atomization. The thermal properties of the Ch12MF4 steel in the dependence on temperature (Figure 3) were defined on the base of their computation by JMatPro software [15] and dilatometry, differential thermal analysis (DTA) and laser flash (LFA) measurements.

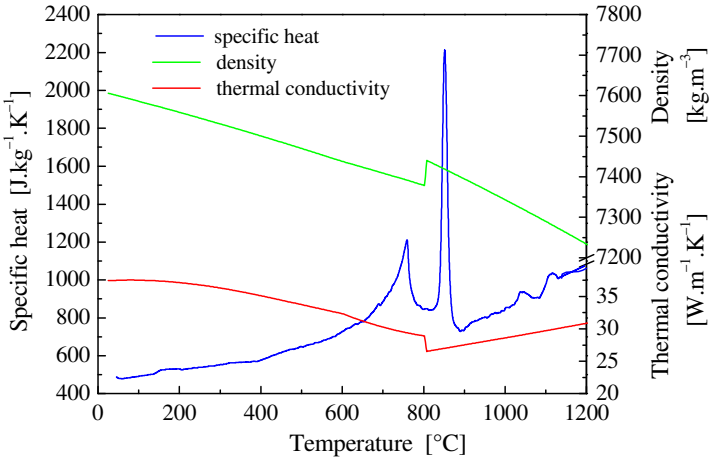

Figure 3. Thermal properties of the Ch12MF4 steel in the dependence on temperature.

The estimation of nucleation temperature T_N based on the Eq. (6) derived from the assumption that the droplet solidification started in the moment when one nucleus of critical size had been formed. According to this equation, the nucleation temperature depends on the cooling rate and the steady-state volumetric nucleation rate. The cooling rate is strongly dependent on the droplet diameter and the heat transfer coefficient governed by the relative velocity of a droplet and atomizing gas [20]. In Figure 4, the maximum cooling rate is plotted as a function of droplet diameter for chosen initial gas velocities representing the different possible positions of a droplet in atomizing conus. The smaller droplets are cooled more intensive thus they can reach deeper undercoolings below the equilibrium liquidus temperature prior to nucleation in comparison with larger droplets.

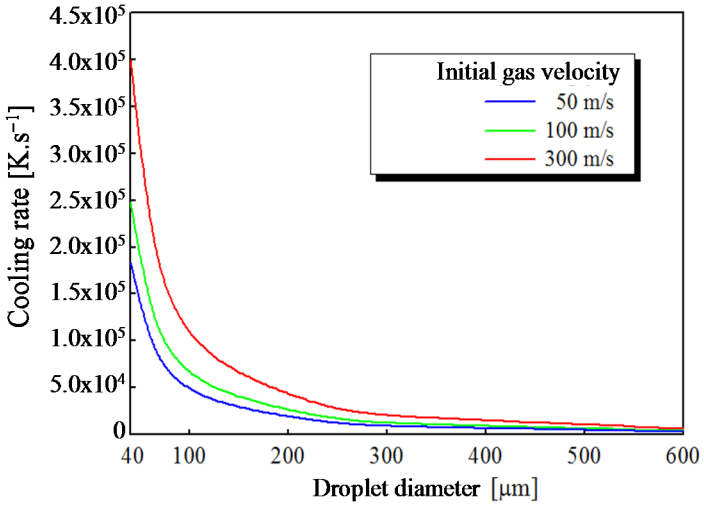

Figure 4. Maximum cooling rate *v.s.* the droplet diameter for different initial velocities of atomizing gas.

The steady-state volumetric nucleation rate is influenced particularly by the solid/liquid interfacial energy, dynamic viscosity and the Gibbs free energy difference between solid and liquid phases. The dependence of the solid/liquid interfacial energy and the viscosity on the melt undercooling is shown in Figure 5. The viscosity enhances by several orders with the increase in droplet undercooling. On the other hand the surface tension for deeper undercoolings decreases.

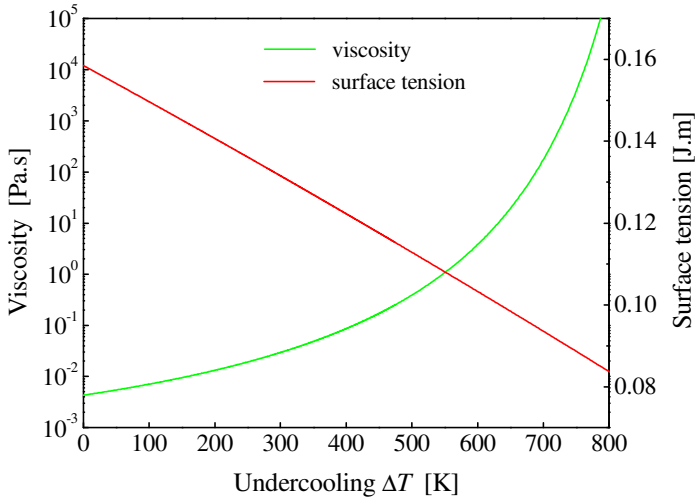

Figure 5. Dependence of the dynamic viscosity and the surface tension on the droplet undercooling.

The dependence of the Gibbs free energy difference ΔG_v computed according the approximations introduced in Table 2 on the droplet undercooling is depicted in Figure 6. As it follows from this figure, for the small undercoolings (up to approximately 50 K), considered relationships results in similar values of ΔG_v. However, the deviations of the Gibbs free energy differences determined according to selected approximations are getting to increase apparently for higher undercoolings. The simple formula suggested by Turnbull provides the upper estimation for the value of the Gibbs free energy difference between solid and liquid phases. The lowest values of ΔG_v were computed applying the Dubey and Ramachandrarao approximation proposed particularly for the glass forming alloys and organic liquids.

In Figure 7, computed temperatures of homogeneous nucleation are plotted as a function of droplet diameter. The maximal nucleation temperature (or in other words the minimal initial undercooling) was calculated for all investigated diameters of droplets using the Turnbull approximation of ΔG_v.

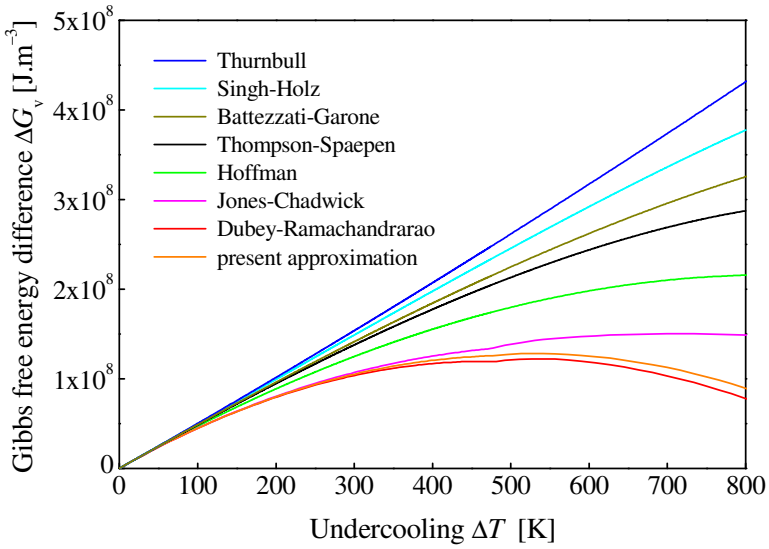

Figure 6. Dependence of the Gibbs free energy difference ΔG_v computed according the approximations introduced in Table 2 on the melt undercooling.

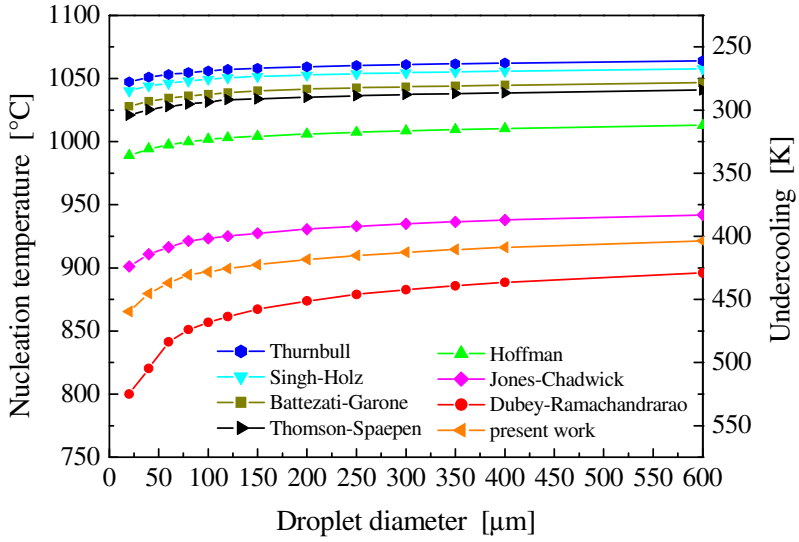

Figure 7. Dependence of the nucleation temperature and initial undercooling on the droplet diameter.

The lowest values of nucleation temperature were provided by the Dubey and Ramachandrarao relationship. In addition, in this case the droplet diameter has higher influence on the computed nucleation temperature. The differences between the nucleation temperatures predicted for droplets with the diameter of 20 μm and 600 μm are larger comparing with those computed using Turnbull formula. Nucleation temperatures computed in the framework of our research by direct application of the Eq. (11) are closer to bottom limit suggested by Dubey and Ramachandrarao. The upper and bottom limits of nucleation temperature and initial undercooling together with values computed by presented model are summarized in Table 3. For the droplets with the largest considered diameter of 600 μm, the initial undercoolings prior to nucleation can reach the values from 260 K (Turnbull approximation) to 428 K (Dubey-Ramachandrarao approximation) corresponding to the nucleation temperatures of 1064 °C and 896 °C, respectively.

Table 3. Nucleation temperature T_N and initial undercooling ΔT_N computed using different approximations of ΔG_v for selected diameters of droplets.

Approximation of ΔG_v	**Droplet diameter**							
	20 μm		**80 μm**		**120 μm**		**600 μm**	
	T_N [°C]	ΔT_N [K]	T_N [°C]	ΔT_N [K]	T_N [°C]	ΔT_N [K]	T_N [°C]	ΔT_N [K]
Turnbull (upper limit)	1047	276	1055	269	1057	267	1064	260
Dubey (bottom limit)	800	524	851	473	861	463	896	428
Current work	865	459	895	429	899	425	921	403

In compliance with the time–temperature–microstructure model of the microstructure development in the rapidly solidified powder particles from Ch12MF4 steel [18], the microstructure transition from dendritic to compound and cellular can occurs if both from following conditions are fulfilled:

- the recalescence temperature is higher then the equilibrium temperature of the eutectic reaction T_{El}=1253 °C and
- the duration of the quasi-isothermal plateau above the T_{El} temperature is sufficiently long.

Figure 8 illustrates the thermal history of a droplet with the diameter of 80 μm rapidly solidifying from different supposed nucleation temperatures and conditions of cooling by nitrogen with the initial velocities of 50 m.s^{-1} and 300 m.s^{-1}, respectively.

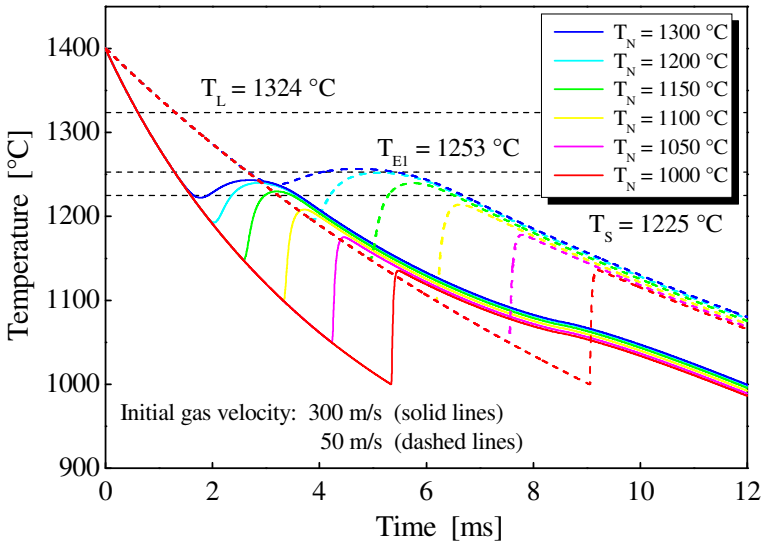

Figure 8. Thermal history of a droplet with the diameter of 80 μm rapidly solidifying from different supposed nucleation temperatures T_N.

If the initial gas temperature is 300 m.s^{-1}, the recalescence temperature does not reach the equilibrium temperature of the eutectic reaction T_{E1}=1253 °C for any assumed nucleation temperature. However, in case of lower initial gas velocity 50 m.s^{-1} and nucleation temperatures above approximately 1200 °C, the first condition for microstructure transition is attained. This finding corresponds to results of microstructural analysis and to the increase in percentage population of cellular and mainly compound microstructures presented in Figure 2.

Figures 9 and 10 show in more details the influence of nucleation temperature and the initial gas velocity on the recalescence temperature and on the duration of the phase of quasi-isothermal solidification for droplets with the diameter of 40 µm, 80 µm, 120 µm and 600 µm.

For the smallest droplet with the diameter of 40 µm, the maximum recalescence temperature attain values bellow or only around the equilibrium solidus temperature (Figure 9). In this reason, the thermally induced fragmentation of dendrites is improbable. The temperature of droplets with the diameter of 80 µm reach the temperature T_{E1} for the nucleation temperatures higher than 1220 °C only in the case of less intensive cooling conditions (initial gas velocity of 50 m.s^{-1}). For these nucleation temperatures, the

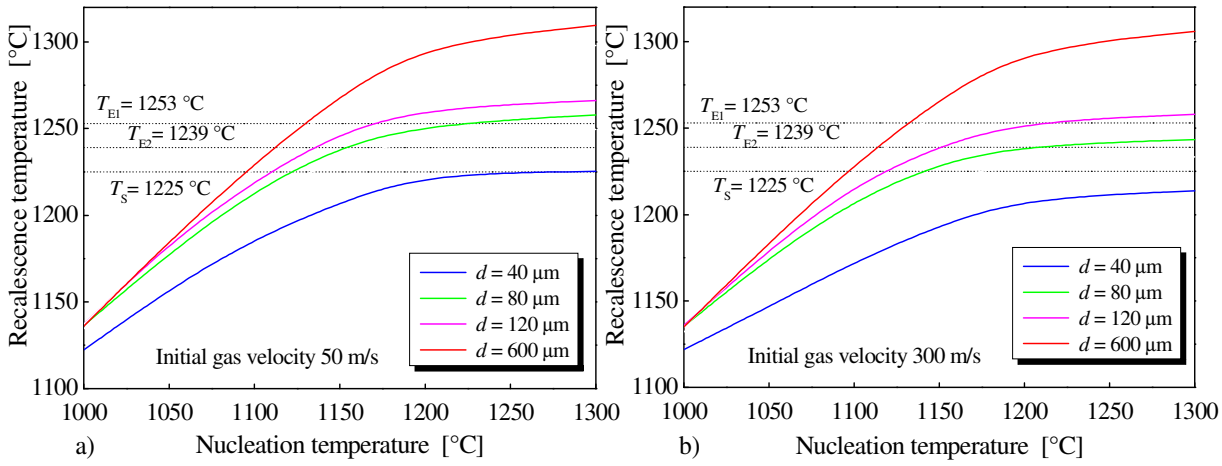

Figure 9. Dependence of recalescence temperature on the nucleation temperature for chosen particle diameters and the initial gas velocity of a) 50 m.s^{-1} and b) 300 m.s^{-1}.

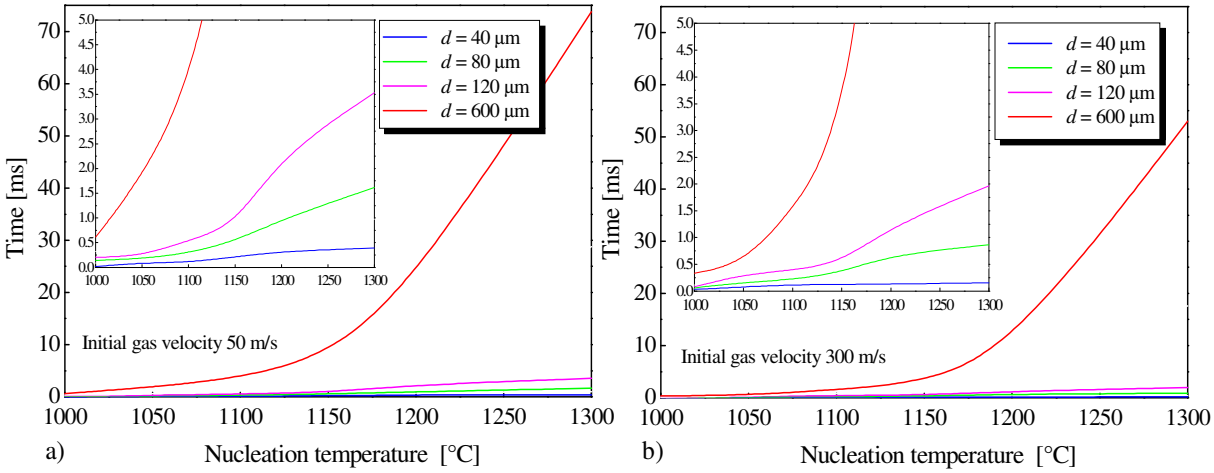

Figure 10. Dependence of the duration of quasi-isothermal plateau on the nucleation temperature for chosen particle diameters and the initial gas velocity of a) 50 m.s^{-1} and b) 300 m.s^{-1}.

duration of quasi-isothermal plateau is more than 1.1 ms. Temperatures in droplets with the diameter of 120 μm rise above the temperature T_{E1} also for the initial gas velocity of 300 m.s^{-1} if the nucleation temperature is higher than 1213 °C or for the nucleation temperatures above 1170 °C when the initial gas velocity is 50 m.s^{-1}. Duration of the quasi-isothermal plateau is 1.2 ms and 1.5 ms, respectively. As the population of compound and cellular microstructures significantly increases in the powder particles larger than 120 μm in diameter (Figure 2), it can be supposed that above mentioned conditions can be sufficient for the initiation of thermally induced fragmentation dendrite and spheroidization of dendrite fragments.

The highest recalescence temperatures and the longest periods of quasi-isothermal solidification are attained in the largest droplets. However, the recalescence temperatures of droplets with the diameter of 600 μm are below the solidus temperature if the nucleation temperatures are lower than approximately 1095 °C. For the nucleation temperatures less than 1130 °C, the recalescence temperatures do not reach the temperature of the eutectic reaction T_{E1}. Under these conditions, the austenite dendrites developed in the phase of recalescence remain unchanged (thermally not influenced) and the final microstructure of solidified particle is dendritic. According computed temperatures of homogeneous nucleation (Table 3), also the largest molten droplets from Ch12MF4 steel can be undercooled below the temperature of 1130 °C and even below the temperature of 1095 °C. This conclusion can be confirmed by the fact that in largest granullometric fractions of RS powder, the percentage population of dendritic microstructure was found to be 34.6 % (Figure 2).

Finally, the computed results were compared with the nucleation temperatures measured in the samples from the tool steel K190 Isomatrix during levitation experiments in the Leibniz Institute for Solid State and Materials Research in Dresden [33-34]. Together 11 samples with the diameters from 6 mm to 8 mm were prepared and treated during 59 experiments. Samples were heated and melted in the vacuum chamber and then cooled by inert gas in electromagnetic levitation or splat quenched on Cu, Sn-Cu or Pb-Cu substrates. The temperatures of spontaneous nucleation along with recalescence temperatures were measured. The melt undercoolings from 50 °C to 290 °C below the equilibrium liquidus temperature were achieved (Figure 11). The spontaneous solidification of samples started the most frequently at undercoolings from 200 °C to 250 °C. Computed results are in a good agreement with the experiments. Measured levels of undercooling correspond approximately to the upper limit of undercooling computed according to Turnbull formula. Taking into account the smaller volumes of droplets and the higher cooling rates acting during gas atomization process, the lower temperatures of homogeneous nucleation computed by the present model or other considered approximations (Table 2) can represent very probable estimation of actual levels of droplet undercooling.

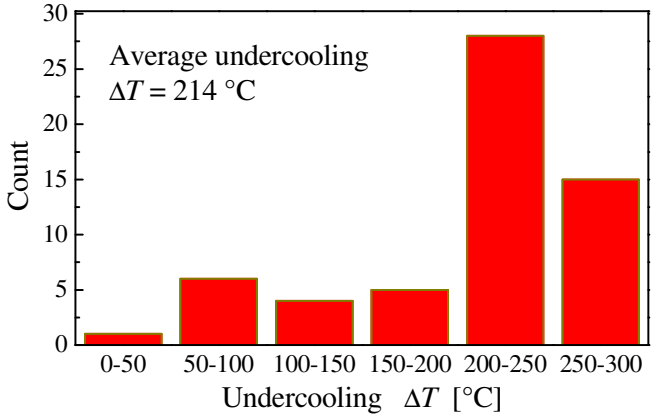

Figure 11. Histogram of achieved undercoolings prior to spontaneous nucleation in levitation experiments [33].

6. Conclusions

Based on the microstructural analysis, computational results and levitation experiments, the following conclusions regarding nucleation and microstructure development during rapid solidification of undercooled droplets from the Ch12MF4 tool steel in the nitrogen gas atomization can be made:

- According to the morphology of austenite, three main types of solidification microstructures were identified in RS powder particles from Ch12MF4 steel - dendritic, compound and cellular (grain-refined).
- Dendritic microstructure was observed in all investigated granullometric fractions of RS powder and its percentage population decreased for larger particles. Statistically significant appearance of compound and cellular microstructures was identified in granullometric fraction from 71-80 μm but considerable enhancement of their proportion was from the granullometric fraction from 125-168 μm.
- It is supposed that the transition from dendritic to compound and cellular microstructure occurs by the mechanism of thermally induced fragmentation of austenite dendrites developed in the phase of recalescence during the quasi-isothermal period of solidification.
- Microstructure transition can occur when the recalescence temperature is higher than both eutectic temperatures and the duration of quasi-isothermal plateau is sufficiently long. Both these parameters are significantly influenced by nucleation temperature.
- Attainable undercooling of molten droplets during gas atomization was predicted using the theory of homogeneous nucleation at the level from 260 K to 524 K.
- During levitation experiments, the most frequently the undercoolings from the interval from 200 K to 250 K were achieved.
- According to computed results, the conditions for microstructure transitions can be fulfilled for particles larger than 80 μm in diameter and mainly for particles with diameter more than 120 μm.
- Dendritic microstructure in largest particles with diameter of 600 μm can remain unchanged if the nucleation temperature is below 1130 °C.

Acknowledgement

The research has been supported by the Scientific Grant Agency of the Slovak Republic (VEGA) within the project No. 1/0811/14, the project No. 1/1010/16 and the project ITMS 26220120048 under the Research & Development Operational Programme funded by the ERDF.

References

[1] Herlach D M 1994 Non-equilibrium solidification of undercooled metallic melts *Mat Sci Eng R* **2** 4–5 177-272.
[2] Rafii-Tabar H and Chirazi A 2002 Multi-scale computational modelling of solidification phenomena *Phys Rep* **365** 3 145-249.
[3] Mondal K and Murty B S 2006 Prediction of maximum homogeneous nucleation temperature for crystallization of metallic glasses *J Non-Cryst Solids* **352** 50–51 5257-5264.
[4] Jia F, Zhao D and Wang M 2016 Selective nucleation and self-organized crystallization *Prog Cryst Growth* **62** 2 252-272.
[5] Perepezko J H and Wilde G 2016 Melt undercooling and nucleation kinetics *Curr Opin Solid State Mater Sci* **20** 1 3-12.
[6] Karma A and Tourret D 2016 Atomistic to continuum modeling of solidification microstructures *Curr Opin Solid State Mater Sci* **20** 1 25-36.

[7] Jacobson L A and McKittrick I 1994 Rapid solidification processing *Mater Sci Eng* **R11** 8 355-408.
[8] Herlach D, Galenko P and Holand-Moritz D 2007 *Metastable solids from undercooled melts* Pergamon Press Amsterdam ISBN 978-0-08-04368-8
[9] Herlach D M 2014 Non-Equilibrium Solidification of Undercooled Metallic Melts *Metals* **4** 2 196-234 doi:10.3390/met4020196
[10] Perepezko J H, Hockel P G and Paik J S 2002 *Termochim Acta* **388** 129-141
[11] Perepezko J H and Hildal K 2008 Metallic glass formation reactions and interfaces *Mater Sci Eng B* **148** 171-178
[12] Perepezko J H 2005 Nucleation controlled phase selection during solidification *Mater Sci Eng A* **413–414** 389-397
[13] Clavaguera-Mora M T et al 2002 *Prog Mater Sci* **47** 559-618
[14] Thermo-Calc Version 2017a. http://www.thermocalc.com
[15] JMatPro, Sente Software Ltd., Surrey Technology Centre, Surrey GU2 7YG, United Kingdom.
[16] Behúlová M, Moravčík R, Kusý L, Čaplovič Ľ, Grgač P and Stanček L 2001 Influence of atomisation on solidification microstructures in the rapidly solidified powder of the Cr-Mo-V tool steel *Mater Sci Eng* **A304-306** 540-543
[17] Grgač P, Behúlová M, Moravčík R and Mesárošová J 2012 *Mater Research* **15** 705-712.
[18] Behúlová M, Mesárošová J and Grgač P 2014 Analysis of the influence of the gas velocity, particle size and nucleation temperature on the thermal history and microstructure development in the tool steel during atomization *J Alloys Compd* **615** 217-223.
[19] Incropera F P, Dewitt D P 1996 *Fundamentals of heat and mass transfer* J Wiley and Sons New York, 1996.
[20] Behúlová M 2005 Influence of initial nitrogen gas velocity on the microstructure development od Ch3F12 alloy in atomization process *Metallic materials* **43** 2 145-157
[21] Perepezko J H 1985 In Proc. of NATO Adv. Research Workshop on RS Technologies, Theuern
[22] Turnbull D 1952 Kinetics of Solidification of Supercooled Liquid Mercury Droplets *J Chem Phys* **20** 411
[23] Thompson C V and Spaepen F 1983 Homogeneous crystal nucleation in binary metallic melts *Acta metall* **31** 12 2021-2027
[24] Turnbull D 1950 Phase Changes *J Appl Phys* **21**1022
[25] Mondal K, Kumar A, Gupta G and Murty B S 2009 Temperature and structure dependency of solid–liquid interfacial energy *Acta Mater* **57** 3422–3430
[26] Turnbull D 1956 *Solid St Phys* Academic Press New York **3** 225
[27] Hoffman J D 1958 Thermodynamic Driving Force in Nucleation and Growth Processes *J Chem Phys* **29** 1192
[28] Thompson C V and Spaepen F 1979 On the approximation of the free energy change on crystallization *Acta Metall* **27** 1855
[29] Battezzati L and Garrone E 1984 *Z Metallkunde* **75** 305
[30] Jones D R H and Chadwick G A 1971 An expression for the free energy of fusion in the homogeneous nucleation of solid from pure melts *Phil Mag* **24** 995
[31] Dubey K S and Ramachandrarao P 1984 On the free energy change accompanying crystallisation of undercooled melts *Acta Metall* **32** 91
[32] Singh H B and Holz A 1983 Stability limit of supercooled liquids *Solid State Communications* **45** 985
[33] Grgač P, Lipták M, Behúlová M, Čaplovič Ľ, Lindenkreuz H-G and Löser W 2007 Influence of melt undercooling on the microstructure of levitated Cr–Mo–V tool steel *Mat Sci Eng A* **449-451** 658-661
[34] Behúlová M, Lipták M, Grgač P, Löser W amd Lindenkreuz H-G 2009 Comparison of microstructures developed during solidification of undercooled tool steel in levitation and on a substrate *Journal of Physics: Conference Series* **144** 1-4